ISBN: 978-3-95450-240-0 ISSN: 2673-5539 doi:10.18429/JACoW-RuPAC2021-MOY02

NICA ION COLLIDER AT JINR

E. Syresin, N. Agapov, A. Alfeev, V. Andreev, A. Baldin, A. Bazanov, O. Brovko, V. Bugaev, A. Butenko, A. Galimov, I. Gorelyshev, D. Donets, E.D. Donets, E.E. Donets, A. Eliseev, G. Filatov, V. Fimushkin, B. Golovenskiy, E. Gorbachev, A. Govorov, A. Grebentsov, E. Ivanov, V. Karpinsky, V. Kekelidze, A. Kirichenko, H. Khodzhibagiyan, A. Kobets, V. Kobets, A. Konstantinov, S. Korovkin, S. Kostromin, O. Kozlov, K. Levterov, D. Lyuosev, A. Malyshev, A. Martynov, S. Melnikov, I. Meshkov, V. Mikhailov, Yu. Mitrophanova, V. Monchinsky, A. Nesterov, A. Osipenkov, K. Osipov, R. Pivin, A. Philippov, D. Ponkin, S. Romanov, P. Rukojatkin, I. Shirikov, A. Shurygin, A. Sidorin, V. Slepnev, A. Slivin, G. Trubnikov, A. Tuzikov, B. Vasilishin, V.Volkov, Joint Institute for Nuclear Research, Dubna , Russia

Abstract

The Nuclotron-based Ion Collider fAcility (NICA) [1-5] is under construction in JINR. The NICA goals are providing of colliding beams for studies of hot and dense strongly interacting baryonic matter and spin physics. The accelerator facility of Collider NICA consists of following elements: acting Alvarez-type linac LU-20 of light ions at energy 5 MeV/u, constructed a new light ion linac of light ions at energy 7 MeV/u and protons at energy 13 MeV, new acting heavy ion linac HILAC with RFQ and IH DTL sections at energy 3.2 MeV/u, new acting superconducting Booster synchrotron at energy up 600 MeV/u, acting superconducting synchrotron Nuclotron at gold ion energy 4.5 GeV/n and two Collider storage rings with two interaction points. The status of acceleration complex NICA is under discussion.

INJECTION ACCELERATOR COMPLEX NICA FOR HEAVY ION MODE

The injection accelerator complex NICA for heavy ion mode [2] involves following accelerators: a new heavy-ion linear accelerator (Heavy Ion Linac, HILAC) constructed by JINR-Bevatech collaboration is under exploitation since 2016. It will accelerate heavy ions such as $^{197}Au^{31+}$ and $^{209}Bi^{35+}$ injected from KRION-6T, a superconducting electron-string heavy ion source, constructed by JINR. At present time KRION-6T produces $8{\cdot}10^8$ Au^{31+} ions and $9{\cdot}10^8$ $^{209}Bi^{35+}$ ions during three pulses of extracted beam. This ion source will be used at injection in Booster in 2022. Upgraded version of KRION-N with $^{197}Au^{31+}$ or $^{209}Bi^{35+}$ion intensity up $2.5{\cdot}10^9$ particles per pulse will be constructed in 2022 for Collider experiments. The energy of ions at the exit from HILAC is 3.2 MeV/n, while the beam intensity amounts to $2{\times}10^9$ particles per pulse or 10 emA, repetition rate is 10 Hz. The HILAC consists of three sections: RFQ and two IH sections. The RFQ is a 4-rod structure operating at 100.625 MHz. The RFQ and each IH section are powered by 140 kW and 340 kW solid state amplifiers. The acceleration of $^{12}C^{2+}$ ions with mass-charge ratio of A/Z=6, produced in laser ion source, was performed at first HILAC tests. Especially for the test run of the Booster the plasma source generating a single component $^4He^{1+}$ (A/Z = 4) beam was created. The maximal ion $^4He^{1+}$ beam current at HILAC entrance during first Booster runs corresponds to project value 10 mA, efficiency of beam transportation through second and third IH sections was 78.5%. During second Booster run the $^4He^{1+}$and $^{56}Fe^{14+}$ ions produced in plasma and laser ion sources were accelerated in HILAC and injected in Booster.

The transfer line from HILAC to Booster [*2*] (Fig. 1) consists of 2 dipole magnets, 7 quadrupole lenses, 6 steerers magnets, debuncher, collimator, vacuum and diagnostic equipment. The transfer line from HILAC to Booster was under operation since autumn 2020. The achieved efficiency of the beam transmission in HILAC – Booster transfer line was about 90% at the beam current of 4 mA.

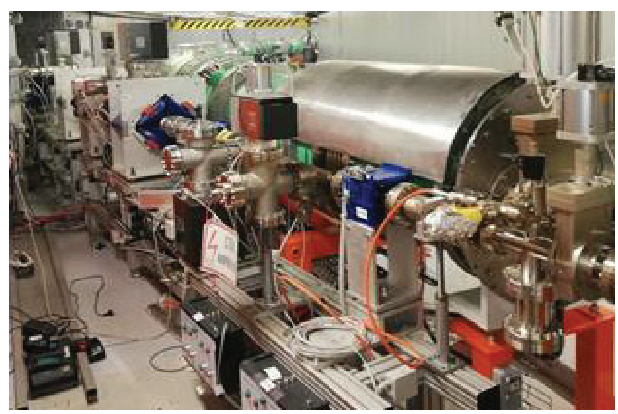

Figure 1: Transport channel HILAC-Booster.

The Booster [1-5] is a superconducting synchrotron intended for accelerating heavy ions up to energy of 578 MeV/u. The magnetic structure of the Booster with a 211 m - long circumference is mounted in tunnel inside the huge iron yoke of the Synchrophasotron magnet (Fig. 2). The main goals of the Booster are accumulation of $2{\cdot}10^9$ $^{197}Au^{31+}$ or $^{209}Bi^{35+}$ ions, acceleration of heavy ions up to the energy 578 MeV/u required for effective stripping, and forming of the required beam emittance with the electron cooling system.

27th Russian Particle Acc. Conf. RuPAC2021, Alushta, Russia JACoW Publishing
ISBN: 978-3-95450-240-0 ISSN: 2673-5539 doi:10.18429/JACoW-RuPAC2021-MOY02

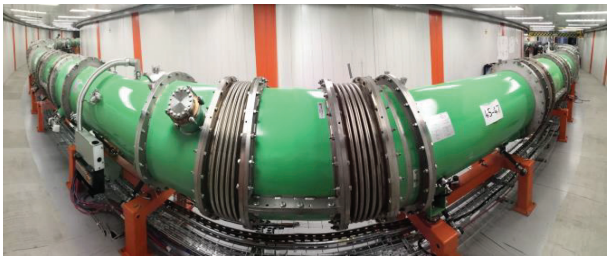

Figure 2: Booster ring in the tunnel inside the Synchrophasotron iron yoke.

The Booster operation was started in end of 2020 [6,7]. The circulated in Booster ion $^{4}He^{1+}$ beam at intensity $7{\times}10^{10}$ corresponds to equivalent project intensity $2{\cdot}10^{9}$ $^{197}Au^{31+}$ ions. During second run in September 2021 the beams of ions $^{4}He^{1+}$ and $^{56}Fe^{14+}$ with mass-charge ratio A/Z=4 and intensity up $4{\cdot}10^{10}$ and $4{\cdot}10^{8}$ correspondently were injected in Booster, bunched on the injection table of magnetic field on fives RF harmonic and then accelerated up energy 65 MeV/n, where they were rebunched on first RF harmonic and again accelerated. The $^{56}Fe^{14}$ ions were accelerated up energy of 578 MeV/n.

The Booster beam extraction system [2] consists of a magnetic kicker, two magnetic septa, a stripping station and a closed orbit bump subsystem including four lattice dipoles with five additional HTS current leads. The Booster beam extraction system together with transfer line Booster Nuclotron (Fig. 3) was fabricated by BINP SB RAS. The first beam experiments with extracted $^{4}He^{1+}$ and $^{56}Fe^{14+}$ ion beams were performed during second Booster beam run.

Figure 3: The transfer line Booster – Nuclotron.

The installation in Nuclotron of beam injection system from the Booster and fast extraction system in Collider [2] are required for its operation as the main synchrotron of the NICA complex. The installation of kickers and Lamberson magnets for Nuclotron injection section is planned in autumn 2021. The operation of Collider NICA injection chain HILAC-Booster-Nuclotron is planned in December 2021-January 2022.

The magnetic system of room-temperature transfer lines from Nuclotron to Collider rings [2,5] was fabricated by French company Sigma Phi. The transfer line lattice contains 27 dipoles, 28 quadrupoles, 33 steerers and set of beam diagnostics devices. The installation of magnet is planned to start in end of 2021. The channel magnets are powered in pulsed mode. The power supplies of magnets will be delivered in JINR in summer 2022.

COLLIDER RINGS

The Collider [1-5] consists of two storage rings with two interaction points (IPs). Its main parameters (Table 1) are as follows: the magnetic rigidity is up to 45 T·m; the residual gas pressure in the beam chamber is not high than 10^{-10} Torr; the maximum field in dipole magnets is 1.8 T; the kinetic energy of gold nuclei ranges from 1 to 4.5 GeV/n; the beam axes coincide at the interaction section (zero intersection angle); and the average luminosity is 10^{27} cm^{-2} s^{-1} for gold ions. The rings of the Collider are identical in shape to a racetrack — two arcs are connected by two long straight section (109 m each). The circumference of each ring is 503.04 m.

The dipole magnets (Fig. 4) and lenses in the arcs are combined into 12 cells of the so-called FODO structure separated by straight sections. The total number of the horizontal dipole magnets in the arcs of both rings corresponds to 80 and 8 vertical dipole magnets for two IP regions. The magnets of both rings in the arcs are situated one above another; their axes are separated vertically by 320 mm. Upon passing the section bringing them together, the particle bunches along the upper and lower rings travel along a common straight trajectory toward each other to collide at two interaction points (IPs). The magnets in the arcs have common yokes, but their construction permits controlling the field in each of the rings separately.

Figure 4: Collider dipole magnet.

ISBN: 978-3-95450-240-0 ISSN: 2673-5539 doi:10.18429/JACoW-RuPAC2021-MOY02

Table 1: Main Parameters of the NICA Accelerator Complex

Parameter	Value		
Ring circumference, m	503,04		
Number of bunches	22		
Rms bunch length, m	0.6		
Beta-function in the IP, m	0.6		
Betatron tunes, Q_x/Q_y	9.44/9.44		
Ring acceptance, π·mm·mrad	40		
Longitudinal acceptance	±0.01		
Ion energy, GeV/n	1	3	4.5
Ion number per bunch	$3.2\cdot10^8$	$2.9\cdot10^9$	$3.1\cdot10^9$
Rms dp/p, 10^{-3}	0.55	1.15	1.5
Rms emittance, π·mm·mrad	1.3/1.3	1.3/1.1	1.3/1.0
Luminosity, $cm^{-2}s^{-1}$	$0.8\cdot10^{25}$	$0.8\cdot10^{27}$	10^{27}
IBS growth time, sec	160	460	2000

The all arc dipole magnets were produced and tested on a cryogenic test bench. The results of cryogenic tests are given in Fig. 5. The measurements of magnet effective length are illustrated by Fig. 6.

The total number of the lenses is equal to 86 in the arcs and the straight sections and 12 lenses of final focus sections. Single-aperture lenses are installed along final focus sections to provide that both beams are focused at the IP.

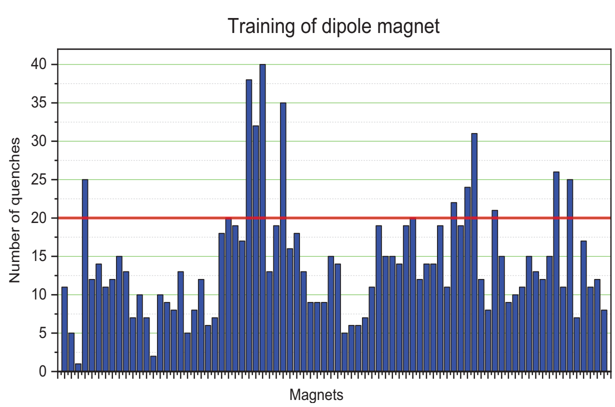

Figure 5: Cryogenic training of dipole magnets.

Three power supplies are used in Collider for all dipole magnets and quadrupole lenses. The Collider main power supply provides consecutive connection of dipole magnets, quadrupole focusing and defocusing lenses at maximum current of 10.7 kA. The second power supply is used for all lenses, and third one is intended only for D lenses. The powers of second and third power supplies are by one order less than power of main power supply. At transition from working point 9.44 to 9.1 the power supply current is variated in all quadrupole lenses on -300 A (except lenses of final focuses) and on 9A for D-lenses. The length of each pair of quadrupole lenses was optimized in straight sections for this case. Additionally, each pair of lenses in straight section and each final focus lens has individual power supply with correction current up 300A.

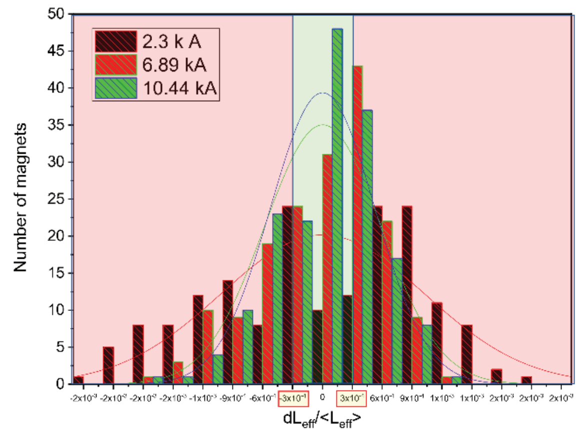

Figure 6: Arc dipole magnet distribution related to their effective lengths.

Methods for cooling of charged particle beams represent the key accelerator technologies, which are critical for achieving the design parameters of the complex. The electron cooling system [2] for the NICA Collider at an electron energy of 2.5 MeV is intended for accumulation and bunch formation at the ion kinetic energies in the range of 1.0–4.5 GeV/n. Construction of the electron cooling system was started in BINP SB RAS in 2016. The assembling of cooling system in JINR will be started in winter 2022.

Table 2: Electron Cooling Parametetrs

Parameter	Value
Electron energy, MeV	0.2 – 2.5
Energy instability, ΔE/E	$\leq 1\cdot10^{-4}$
Electron beam current, A	0.1 – 1.0
Cooling section length, m	6.0
Solenoid magnetic field, T	0.05 – 0.2
Field inhomogeneity, ΔB/B	$\leq 1\cdot10^{-5}$

The main goal of using stochastic cooling system (SCS) in colliding ion beam experiments in the Collider NICA is to achieve and maintain design luminosities of $10^{27}cm^{-2}c^{-1}$ in the beam energy range from 3 to 4.5 GeV / u. The stochastic cooling system [2] of the NICA Collider must provide ion cooling of up to $3.1\cdot10^9$ ions in a bunch, which corresponds to an effective number $8\cdot10^{11}$ of ions. To achieve the design cooling time, an SCS with the frequency bandwidth 0.7–3.2 GHz is necessary. The SCS is a broadband microwave feedback system via the beam and in the main configuration consists of 6 channels for longitudinal, horizontal and vertical cooling, respectively for each Collider ring. In the basic configuration, the SCS consists only

ISBN: 978-3-95450-240-0 ISSN: 2673-5539 doi:10.18429/JACoW-RuPAC2021-MOY02

of longitudinal cooling channels. Each channel has the following main components: pickup, cascade of preamplifiers, signal transmission lines, electronics for control, power amplifiers, kicker. As pickups and kickers, a ring structure with a slot coupling is taken as the basis. The unit cell of this structure is a ring with eight azimuthally distributed sensor loops Several rings are combined by microstrip boards, summing the signal in each of the azimuthal directions.

Table 3: Stochastic Cooling Parametetrs

Longitudinal cooling method	Filter
Passband, GHz	0.7 – 3.2
Beam distance from pickup to kicker, m	183.5-191.5
Phase advance from pickup to kicker, deg	1340-1360
Ion energy $^{197}Au^{79+}$, GeV/u	3.0
Slip-factor from pickup to kicker	0.0294
Revolution slip-factor	0.0362
Pickup/kicker coupling impedance, Ω	200/800
Gain, dB	75 – 79
Peak power at kicker, W	3·200
Pickup/noise temperature, K	300/40

Three RF systems with 26 cavities of the acceleration radio-frequency voltage will be applied for ion accumulation and formation of ion bunches [2,5] with the necessary parameters in the Collider. Accumulation of the beam of the required intensity is planned to be realized in the longitudinal phase space with the use of the 'technique of barrier RF1 voltages' (Fig. 7) and of stochastic or electron cooling of the particles being accumulated. The burrier bucket technique also will be used for ion acceleration in the rings

The RF1 system generates 2 pairs of ±5 kV pulses (accelerating and decelerating in each pair) at the bunch revolution frequency thus forming two separatrices – injection and stack. A bunch from the Nuclotron is captured into the injection separatrix, circulates in the ring until wo pulses separating separatrices are switched off and the injected bunch merges with the stack. The accumulated ions trapped between the two barrier pulses may be accelerated, if necessary, by ±0.3 kV meander voltage generated by the RF1 as well. The RF1 system is actually an induction accelerator composed by 20 inductor sections: 15 are used to form the barriers, 3 generate accelerating meander voltage and 2 passive damping sections correct voltage shape. Each active section is driven by a pair of pulse generators. An inductor section consists of a magnetic core made from the amorphous magnetic alloy and glued between the two water cooled copper plates.

Figure 7: Burrier bucket RF1 cavity.

When the necessary ion intensity is achieved, the beam is bunched the RF2 system (Table 4, Fig. 8) at voltage up to 25 kV of the 22nd harmonics of the rotation frequency with the subsequent takeover by the RF3 system (Table 4) of the 66th harmonics. This permits 22 short bunches to be formed, which is necessary in order to achieve high luminosity. The maximal RF3 voltage corresponds to 125 kV. The RF2 and RF3 systems additionally will be used for an ion acceleration in rings from injection energy up to energy required for Collider experiments. The RF2 and RF3 cavities are of coaxial type which makes the cavity diameter small enough to fit in between the two Collider rings separated by 320 mm only. In order to decrease the length down to an acceptable value the cavity is heavily loaded by a mushroom-like capacitor. Due to the wide operating frequency range (12%) the cavity has four capacitive tuners. The RF solid state amplifiers developed by Russian firm TRIADA are used for RF2 and RF3 systems.

Table 4: Parameters of RF2 and RF3 Cavities

Value	RF2	RF3
Harmonic	22	66
Frequency, MHz	11.484÷ 12.914	34.452÷ 38.742
Rsh,Ohms	$3.12{\cdot}10^5$	$2.68{\cdot}10^6$
Q	3900	6700
Rate of cavity frequency variation, kHz/s	14.7	25.7
RF voltage, kV	25	125
Number of cavities per ring	4	8

ISBN: 978-3-95450-240-0 ISSN: 2673-5539 doi:10.18429/JACoW-RuPAC2021-MOY02

The construction of three RF systems was started in 2016-2017 in BINP SB RAS. Two RF1 and four RF2 cavities will be installed in JINR in beginning of 2022. Additional 4 RF2 and 16 RF3 cavities will be commissioned for extension collider version in end of 2022.

Figure 8: Prototype of RF2 cavity.

The beam injection system is designed for single-turn injection of heavy nuclei into Collider rings with minimal losses. Systems' elements are placed inside the cryostat in straight sections located in the arch of the half-ring E of Collider. The main elements of the beam injection system are septum and kicker magnets, as well as a closed-orbit bump subsystem consisting of Collider lattice dipole magnets with additional current leads. Septum magnets are used to enter the beam into the vacuum chambers of the Collider rings. Kicker magnets are used to land the beam onto a closed orbit. In order to weaken the requirements for kicker magnets, the circulating beam is shifted to the knives of the septum magnets of the injection system, for which local closed orbit bumps are created at the beam entry sites in Collider. The beam injection system now is under design, its fabrication and installation is planned in autumn 2022.

The beam dumping from Collider is carried out by a set of kicker and septum magnets mounted symmetrically to the system of beam injection in the ring with the opposite direction of particle motion. The beams are dumped in the directions opposite to the directions of beam injection into Collider rings. Kicker magnets throw circulating beams into septum magnets, which complete the extraction of the beams from the Collider rings. The beam extraction system is designed now, its fabrication is planed in 2022, commissioning of this system should be done in 2023.

The beam diagnostic system (Table 5) involves pick-up electrodes, strip line monitor, current transformers, Q-meter for tune measurements, ionization profile monitor, Schottky pick-up electrodes, beam loss monitor. The diagnostic equipment is under construction; their installation is planned in 2022.

The feedback system is used for suppression of the coherent transverse beam oscillations: damping of coherent transverse oscillations, arising from injection errors, damping of coherent transverse instabilities, excitation of coherent transverse oscillations at betatron tune measurements. The feedback system is under construction; their installation is planned in autumn 2022.

Table 5: Beam Diagnostic System

Pick-up near F lenses (X)	24
Pick-up near D lenses (Z)	24
Pick-up in straight sections (X/Z)	20
Parametric current transformer (Bergoz	1
Fast current transformer (Bergoz)	2
Betatron tune measurements (Q-meter)	1
Ionization profile monitor	3
Schottky pick-up electrode	1
Strip pick-up monitor	2
Beam loss monitors (for both rings)	68

The beam collimation system in each Collider ring consists of foil section for scattering of ions with the large betatron amplitudes and four catchers for x and y coordinates. This system is fabricated now; their installation is planned in end 2022.

REFERENCES

[1] G. V. Trubnikov *et al.,* "Project of the Nuclotron-based Ion Collider Facility (NICA) at JINR", in *Proc. 11th European Particle Accelerator Conf. (EPAC'08),* Genoa, Italy, Jun. 2008, paper WEPP029, pp. 2581-2583.

[2] Technical Project of NICA Acceleration Complex, Dubna, 2015.

[3] V.D. Kekelidze, R. Lednicky, V.A. Matveev, I.N. Meshkov, A.S. Sorin and G.V. Trubnikov, "Three stages of the NICA accelerator complex", *Eur. Phys. J.* A52: 211, 2016.

[4] N.N. Agapov, *et al.*, "Relativistic nuclear physics in JINR: from Synchrophasotron to Collider NICA", *Phys. Usp*., v.59, p. 383. 2016.

[5] E. Syresin *et al.*, "Status of Accelerator Complex NICA", in *Proc. 26th Russian Particle Accelerator Conf. (RuPAC'18)*, Protvino, Russia, Oct. 2018, pp. 12-16. doi:10.18429/JACoW-RUPAC2018-MOXMH03

[6] A. V. Butenko *et al.,* "First Experiments with Accelerated Ion Beams in the Booster of NICA Accelerator Complex", presented at the *12th Int. Particle Accelerator Conf. (IPAC'21),* Campinas, Brazil, May 2021, paper MOPAB025.

[7] A V Butenko, *et.al.,* "Vacuum conditions and beam lifetime of single charged He ions in Booster NICA (first run)", *Exper. Theor. Phys. Letters*, v.113, p.752. 2021.